

Chao, J.; Ram, S.; Ward, E.S.; Ober, R.J., "A 3D resolution measure for optical microscopy," in *Biomedical Imaging: From Nano to Macro, 2009. ISBI '09. IEEE International Symposium on* , vol., no., pp.1115-1118, June 28 2009-July 1 2009
doi: 10.1109/ISBI.2009.5193252

keywords: {bio-optics;biological techniques;cellular biophysics;image resolution;maximum likelihood estimation;molecular biophysics;optical microscopy;3D spatial orientation;Cramer-Rao inequality;biological cell;biomolecules interaction;information-theoretic 3D resolution measure;maximum likelihood estimator;optical microscope;Biological cells;Biomedical optical imaging;Cramer-Rao bounds;Extraterrestrial measurements;Image resolution;Molecular biophysics;Object detection;Optical microscopy;Predictive models;Spatial resolution;Axial resolution;Cramer-Rao inequality;Fisher information matrix;optical microscopy;three-dimensional microscopy},

URL: <http://ieeexplore.ieee.org/stamp/stamp.jsp?tp=&arnumber=5193252&isnumber=5192959>

A 3D RESOLUTION MEASURE FOR OPTICAL MICROSCOPY

Jerry Chao^{1,2}, Sripad Ram², E. Sally Ward², and Raimund J. Ober^{1,2,*}

¹Department of Electrical Engineering, University of Texas at Dallas, Richardson, TX,

²Department of Immunology, University of Texas Southwestern Medical Center, Dallas, TX.

ABSTRACT

An information-theoretic three-dimensional (3D) resolution measure for the optical microscope is introduced. Based on the Cramer-Rao inequality, this resolution measure specifies a lower bound on the accuracy with which a given distance separating two objects in 3D space can be estimated from the acquired image. Useful in many applications, accurate determination of the distance of separation can, for example, help to characterize the interaction that occurs between two closely spaced biomolecules in a biological cell. In addition to presenting the underlying theory, we show that the resolution measure predicts that, by detecting a sufficient number of photons from an object pair, arbitrarily small distances of separation can be estimated with prespecified accuracy. Furthermore, we illustrate its dependence on properties such as the object pair's 3D spatial orientation. With estimations on simulated images, we show that the maximum likelihood estimator is capable of attaining the accuracy predicted by the resolution measure.

Index Terms— Axial resolution, Cramer-Rao inequality, Fisher information matrix, optical microscopy, three-dimensional microscopy

1. INTRODUCTION

The lateral (two-dimensional (2D)) resolution of the optical microscope has been the focus of many studies. There, it is assumed that the two closely spaced objects of interest are both confined to a focal plane of the microscope. In many applications, however, the imaged objects are situated in three-dimensional (3D) space. The advent of single molecule microscopy, for example, has made possible the imaging of biomolecules which interact with one another inside the 3D environment of a biological cell. In this case, the ability to accurately determine the distance of separation between two closely spaced biomolecules can provide invaluable information for characterizing the nature of their association. For applications like such, the task of estimating the distance of separation between two objects is one of resolution in 3D.

In this paper, we consider the 3D resolution of the optical microscope within the context of a parameter estimation problem. By making use of the theoretical framework that is laid out in [1] for formulating a general parameter estimation problem in optical microscopy, we introduce a resolution measure based on the Cramer-Rao lower bound [2] that predicts the accuracy with which a given distance separating two objects in 3D space can be determined.

Analogous to our result in [3] wherein the same mathematical framework is applied to the 2D scenario of a pair of in-focus objects, the 3D resolution measure predicts that, by detecting enough photons from a pair of objects, arbitrarily small distances of separation can be estimated with pre-specified accuracy. In addition to this photon count dependence, we illustrate here the resolution measure's behavior as a function of an object pair's distance of separation, 3D spatial orientation, and location along the optical axis. As it is a lower bound on the accuracy for distance estimation, we also provide results of estimations on simulated images of point source pairs which show the maximum likelihood estimator to be capable of attaining the resolution measure.

The material presented here is a practically significant expansion of what we have previously proposed [4, 5], and represents an important subset of the content of [6]. In Section 2, we present the theory behind the 3D resolution measure. In Section 3, we demonstrate the dependence of the resolution measure on the various attributes of an object pair. In Section 4, we give the results of our estimations on simulated data.

2. THEORY

We consider the parameter estimation problem wherein the unknown parameter vector comprises six parameters that collectively describe the 3D location of an object pair. This vector is given by $\theta = (d, \phi, \omega, s_x, s_y, s_z)$, $\theta \in \Theta$, where the parameter space Θ is an open subset of \mathbb{R}^6 . Illustrated in Fig. 1 for a pair of point sources, s_x , s_y , and s_z are the coordinates of the midpoint of the line segment that joins the two objects, d is the length of the line segment (i.e., the distance of separation), ϕ is the angle between the xy -plane projection of the line segment and the positive x -axis, and ω is the angle between the line segment and the positive optical (z -)axis. In our previous work [4, 5], a less practical assumption was

This work was supported in part by the National Institutes of Health (R01 GM071048 and R01 GM085575). *Corresponding author, email: ober@utdallas.edu.

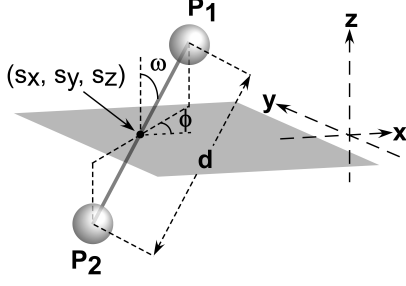


Fig. 1. Pair of point sources situated in 3D space. The point sources are separated by a distance d , with the midpoint between them given by the coordinates (s_x, s_y, s_z) . The orientation of the point source pair is described by the angle ω which the line segment P_1P_2 connecting the pair forms with the positive z -axis, and the angle ϕ which the xy -plane projection of P_1P_2 forms with the positive x -axis.

made in that the distance d was considered the only unknown parameter.

To quantify the accuracy with which a given distance of separation can be determined, we make use of the well-known Cramer-Rao inequality from estimation theory [2]. This inequality states that the covariance matrix of any unbiased estimator $\hat{\theta}$ of the unknown parameter vector θ is no smaller than the inverse of the Fisher information matrix $\mathbf{I}(\theta)$, i.e.,

$$\text{Cov}(\hat{\theta}) \geq \mathbf{I}^{-1}(\theta). \quad (1)$$

Since the distance of separation d corresponds to element $(1, 1)$ of $\mathbf{I}^{-1}(\theta)$, and as it is common to express the accuracy of an estimator in terms of its standard deviation, the 3D resolution measure is defined to be the quantity $\sqrt{[\mathbf{I}^{-1}(\theta)]_{11}}$. The resolution measure is therefore a lower bound on the standard deviation of any unbiased estimator of d . Accordingly, a large resolution measure indicates poor accuracy, while a small resolution measure indicates good accuracy.

To arrive at the Fisher information matrix $\mathbf{I}(\theta)$ for the 3D resolution problem, we start generally by modeling an acquired image in optical microscopy as a spatio-temporal random process, which we refer to as the image detection process [1]. An image of N_p pixels, acquired during the time interval $[t_0, t]$, is modeled as a sequence of independent random variables $\{\mathcal{I}_{\theta,1}, \dots, \mathcal{I}_{\theta,N_p}\}$, where $\mathcal{I}_{\theta,k} = S_{\theta,k} + B_k + W_k$, $k = 1, \dots, N_p$. In the expression for $\mathcal{I}_{\theta,k}$, $S_{\theta,k}$ is a Poisson random variable that denotes the number of photons at the k^{th} pixel that are detected from the objects of interest, and it depends on the unknown parameter vector θ . The random variable B_k is also Poisson-distributed, but represents the number of spurious photons at the k^{th} pixel due to noise sources such as sample autofluorescence. The random variable W_k is a Gaussian random variable that denotes the number of photons at the k^{th} pixel due to measurement noise such as that generated by the detector readout process. The three random variables at each pixel are independent of each other, and we

assume that B_k and W_k , $k = 1, \dots, N_p$, are independent of the unknown parameter vector θ .

It was shown in [1] that the number of photons $S_{\theta,k}$ detected from the objects of interest at the k^{th} pixel is distributed with mean

$$\mu_{\theta}(k, t) = \int_{t_0}^t \int_{C_k} \Lambda_{\theta}(\tau) f_{\theta,\tau}(x, y) dx dy d\tau, \quad (2)$$

where C_k is the region in the xy -plane occupied by the k^{th} pixel, Λ_{θ} is the time varying intensity function of the inhomogeneous Poisson process that models the time points at which the photons are detected, and $\{f_{\theta,\tau}\}_{\tau \geq t_0}$ are the density functions of the sequence of independent random variables that model the spatial coordinates of the detected photons.

If we denote the mean of the number of spurious photons B_k at the k^{th} pixel by $\beta(k, t)$, and the mean and standard deviation of the number of photons W_k due to measurement noise at the k^{th} pixel by η_k and σ_k , respectively, then the Fisher information matrix is given by [1]

$$\mathbf{I}(\theta) = \sum_{k=1}^{N_p} \left(\frac{\partial \mu_{\theta}(k, t)}{\partial \theta} \right)^T \frac{\partial \mu_{\theta}(k, t)}{\partial \theta} \times \left(\int_{\mathbb{R}} \frac{\left(\sum_{l=1}^{\infty} \frac{[\nu_{\theta}(k, t)]^{l-1} e^{-\nu_{\theta}(k, t)}}{(l-1)! \sqrt{2\pi} \sigma_k} \cdot e^{-\frac{1}{2} \left(\frac{z-l-\eta_k}{\sigma_k} \right)^2} \right)^2}{p_{\theta,k}(z)} dz - 1 \right), \quad (3)$$

where the superscript T denotes the transpose operation, and for $k = 1, \dots, N_p$, $\nu_{\theta}(k, t) = \mu_{\theta}(k, t) + \beta(k, t)$, and

$$p_{\theta,k}(z) = \frac{1}{\sqrt{2\pi} \sigma_k} \sum_{l=0}^{\infty} \frac{[\nu_{\theta}(k, t)]^l e^{-\nu_{\theta}(k, t)}}{l!} e^{-\frac{1}{2} \left(\frac{z-l-\eta_k}{\sigma_k} \right)^2}, \quad z \in \mathbb{R}. \quad (4)$$

For the resolution problem at hand, the acquired image is that of a pair of objects, and the parameter vector θ comprises the six parameters described above. Accordingly, we realize $\mu_{\theta}(k, t)$ of Eq. (2) as follows. We define the intensity function of the Poisson process to be the sum of the photon detection rates Λ_1 and Λ_2 of the two objects, i.e., $\Lambda_{\theta}(\tau) = \Lambda_1(\tau) + \Lambda_2(\tau)$, $\tau \geq t_0$. Similarly, the density function $f_{\theta,\tau}$ is a weighted sum of the images of the two objects, and is given by

$$f_{\theta,\tau}(x, y) = \frac{1}{M^2} \left[\epsilon_1(\tau) q_{z_{01},1} \left(\frac{x}{M} - x_{01}, \frac{y}{M} - y_{01} \right) + \epsilon_2(\tau) q_{z_{02},2} \left(\frac{x}{M} - x_{02}, \frac{y}{M} - y_{02} \right) \right], \quad (5)$$

where $(x, y) \in \mathbb{R}^2$, $\epsilon_i(\tau) = \Lambda_i(\tau) / (\Lambda_1(\tau) + \Lambda_2(\tau))$, $i = 1, 2$, $\tau \geq t_0$, M is the lateral magnification of the microscope, (x_{01}, y_{01}, z_{01}) and (x_{02}, y_{02}, z_{02}) are the 3D coordinates, expressed in terms of θ , of the locations (e.g., centers of mass) of the two objects in the object space, and $q_{z_{01},1}$ and $q_{z_{02},2}$ are the image functions of the two objects. An image function q_{z_0} is defined as the image of an object at unit lateral magnification when the object is located at $(0, 0, z_0)$, $z_0 \in \mathbb{R}$, in the object space [1].

3. DEPENDENCE ON OBJECT PAIR ATTRIBUTES

In this section, we illustrate the behavior of the resolution measure as a function of various object pair attributes. We

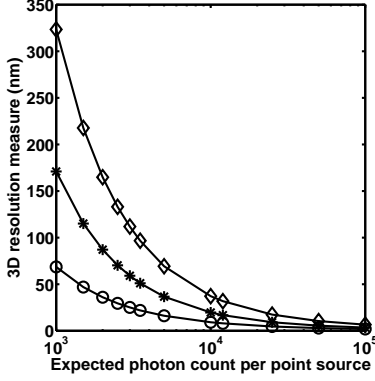


Fig. 2. Dependence of the 3D resolution measure on the expected photon count for three point source pairs that differ only in their distances of separation: $d = 50$ nm (\diamond), 100 nm ($*$), and 200 nm (\circ). In all three cases, the point source pair is axially centered at 350 nm above the focal plane ($s_z = 350$ nm), and is positioned in the xy -plane such that its image is centered on a 21 -by- 21 pixel array with a pixel size of $6.45 \mu\text{m}$ by $6.45 \mu\text{m}$. The orientation is such that the pair projects at a 60° angle from the positive x -axis in the xy -plane ($\phi = 60^\circ$), and forms a 60° angle with the positive optical axis ($\omega = 60^\circ$). Each point source emits photons of wavelength $\lambda = 655$ nm, and the expected photon count $\Lambda_0 \cdot (t - t_0)$ from each is varied from 1000 to 100000 photons. The refractive index of the object space medium is set to $n = 1.515$, and the numerical aperture and magnification of the objective lens are respectively set to $n_a = 1.45$ and $M = 100$. The mean of the additive Poisson noise at each pixel is set to $\beta(k, t) = 80$ photons, and the mean and standard deviation of the additive Gaussian noise at each pixel are set to $\eta_k = 0 e^-$ and $\sigma_k = 8 e^-$, respectively.

consider the important scenario where the object pair is a pair of like point sources that emit photons of the same wavelength and the same constant detection rate (i.e., $\Lambda_1(\tau) = \Lambda_2(\tau) = \Lambda_0$, $\tau \geq t_0$). Furthermore, the image function of each point source is given by the classical 3D point spread function of Born and Wolf [7]. That is, $q_{z_{01},1}$ and $q_{z_{02},2}$ are each of the form

$$q_{z_0}(x, y) = \frac{4\pi n_a^2}{\lambda^2} \left| \int_0^1 J_0 \left(\frac{2\pi n_a}{\lambda} \sqrt{x^2 + y^2} \rho \right) e^{j \frac{\pi n_a^2 z_0}{n \lambda} \rho^2} \rho d\rho \right|^2, \quad (6)$$

$(x, y) \in \mathbb{R}^2$, $z_0 \in \mathbb{R}$. In Eq. (6), n_a denotes the numerical aperture of the objective lens, λ denotes the wavelength of the detected photons, and n denotes the refractive index of the immersion medium.

Dependence on photon count Intuitively, the more photons (i.e., data) that are detected from two point sources, the more accurately one should be able to determine the distance that separates them. This idea is reflected in our resolution measure. Fig. 2 illustrates the photon count dependence of the resolution measure for three point source pairs that differ only in their distances of separation. In each case, the curve shows that the accuracy for distance estimation improves (i.e., the resolution measure decreases) nonlinearly with increasing

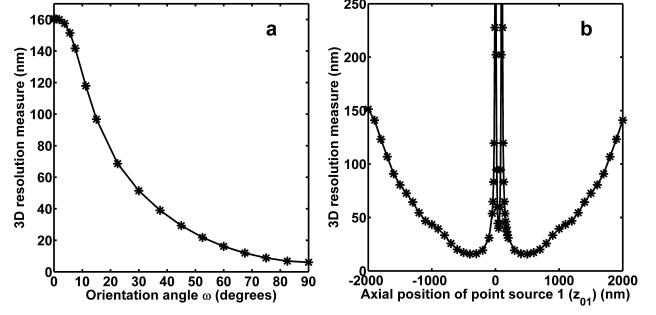


Fig. 3. Dependence of the 3D resolution measure on (a) the 3D orientation (angle ω) and (b) the axial location of a point source pair with a separation distance of $d = 200$ nm and an expected photon count of $\Lambda_0 \cdot (t - t_0) = 5000$ per point source. In (b), the resolution measure is shown as a function of the axial position z_{01} of the first point source, and the focal plane is located at $z_{01} = 0$ nm. In both (a) and (b), all other point source pair attributes and all experimental and noise parameters are as given for Fig. 2, except for the angle ω in (a) and the axial position in (b) which are varied along the x -axes.

expected photon count. For a distance of $d = 200$ nm, for example, the resolution measure predicts an accuracy of ± 29.47 nm when an expected 2500 photons are detected from each point source. By doubling the expected photon count to 5000 photons per point source, the accuracy is improved to ± 16.13 nm. This photon count dependence importantly implies that given enough photons, arbitrarily small distances can be determined with prespecified accuracy.

Dependence on distance of separation By intuition, one would expect that larger separation distances can be determined more accurately than smaller ones, since in the latter case more overlap is expected of the images of the two point sources. Fig. 2 shows that given an expected number of detected photons, the resolution measure for a larger distance is better (i.e., smaller) than that for a smaller distance. For example, by detecting an expected 5000 photons per point source, accuracies of ± 16.13 nm, ± 36.60 nm, and ± 69.34 nm can be expected for estimating distances of 200 nm, 100 nm, and 50 nm, respectively. In terms of percentages, these accuracies correspond to less than 10% , less than 40% , and greater than 100% of the respective distances.

Dependence on 3D orientation Intuitively, one would expect that it would be easiest to determine the distance of separation when two point sources are located side-by-side in an xy -plane ($\omega = 90^\circ$), and that the task would become increasingly more difficult as they are rotated toward the orientation where one point source is positioned directly in front of the other ($\omega = 0^\circ$). As illustrated in Fig. 3a, our resolution measure predicts results that concur. The curve shows that the side-by-side scenario ($\omega = 90^\circ$) corresponds to the best accuracy (i.e., smallest resolution measure), and that as we rotate the point source pair out of and away from the xy -plane

(i.e., decrease the angle ω), we start to lose accuracy slowly but steadily until roughly an angle half way between the xy -plane and the optical axis ($\omega = 45^\circ$) is formed with the optical axis. Then, as the point source pair is rotated further towards the front-and-back orientation ($\omega < 45^\circ$), the deterioration in accuracy becomes significantly sharper before eventually leveling off at very small values of ω .

Dependence on axial location The farther two point sources are from the focal plane, the more they will appear in the acquired image to be a single point source, and hence the more difficult it will be to determine the distance that separates them. This is corroborated by the curve shown in Fig. 3b, which shows how the value of the resolution measure changes as a point source pair is moved along the optical axis from two microns below the focal plane to two microns above. In general, the curve shows that as the point source pair is moved away from the focal plane in either direction along the optical axis, the accuracy for determining the distance of separation worsens.

The exception to the rule for axial locations within half a micron from the focal plane can be explained by the fact that the accuracy with which the axial position of a point source can be determined deteriorates drastically when the point source is near the focal plane [8]. Since the problem of resolving two point sources can be viewed equivalently as determining the locations of the two point sources, this inability to accurately localize a near-focus point source has similar implications for the resolution problem. As shown in Fig. 3b, the ability to accurately determine the distance of separation is severely compromised by either of the two point sources coming very close to the focal plane. Each of the two sharp increases corresponds to one of the point sources being very close to the focal plane.

4. ESTIMATION RESULTS

Since by definition the 3D resolution measure is a lower bound on the standard deviation of any unbiased estimator of the distance of separation, it is practically important to know that there are estimators that can in fact attain the indicated accuracy. By performing estimations on images of pairs of like point sources in 3D space simulated using the image function of Eq. (6), we found that the maximum likelihood estimator is capable of achieving the resolution measure.

The maximum likelihood estimation was realized by maximizing the log-likelihood function

$$\ln(\mathcal{L}(\theta|z_1, \dots, z_{N_p})) = \sum_{k=1}^{N_p} \ln(p_{\theta,k}(z_k)), \quad (7)$$

where for $k = 1, \dots, N_p$, z_k is the simulated photon count at the k^{th} pixel (i.e., $z_k = S_{\theta,k} + B_k + W_k$), and $p_{\theta,k}(z_k)$ is the probability density function of z_k given by Eq. (4).

Using MATLAB (The MathWorks, Inc., Natick, MA) and its optimization toolbox, we performed estimations on five sets of simulated data which differ in parameters such as the distance of separation and the spatial orientation. For each data set, estimations were carried out on 500 images. Table 1 shows that in each of the five scenarios, the mean and standard deviation of the distance estimates closely match the true distance of separation and the resolution measure, respectively. These results therefore demonstrate that the maximum likelihood estimator is capable of achieving the accuracy predicted by the resolution measure.

Table 1. Results of maximum likelihood estimations

Data set no.	Expected photon count per point source	ω (deg.)	s_z (nm)	d (nm)	Mean (nm)	Res. meas. (nm)	Std. dev. (nm)
1	5000	60	350	200	201.08	16.35	16.07
2	7500	60	350	200	200.76	11.71	11.72
3	5000	70	350	200	201.45	10.90	10.35
4	5000	60	450	200	201.29	16.15	16.44
5	5000	60	350	250	250.62	12.17	11.30

Results of maximum likelihood estimations on five sets of 500 simulated images of point source pairs in 3D space. For each data set, the mean and standard deviation of the distance estimates are shown along with the corresponding resolution measure and the values of the parameters that differ between the data sets. For all data sets, the point source pair emits photons of wavelength $\lambda = 655$ nm, has an angle $\phi = 60^\circ$, and is positioned in the xy -plane such that its image is centered on a 15-by-15 array of $6.45 \mu\text{m}$ by $6.45 \mu\text{m}$ pixels. All other experimental and all noise parameters are as given for Fig. 2.

5. REFERENCES

- [1] S. Ram et. al., "A stochastic analysis of performance limits for optical microscopes," *Multidim. Syst. Sig. Process.*, vol. 17, pp. 27–57, 2006.
- [2] C. R. Rao, *Linear statistical inference and its applications*, Wiley, New York, USA., 1965.
- [3] S. Ram et. al., "Beyond Rayleigh's criterion: A resolution measure with application to single-molecule microscopy," *PNAS*, vol. 103, pp. 4457–4462, 2006.
- [4] S. Ram et. al., "A novel 3D resolution measure for optical microscopes with applications to single molecule imaging," *Proc. SPIE*, 64440D, 2007.
- [5] J. Chao et. al., "3D resolution measure for multifocal plane microscopy," in *Proc. 5th IEEE International Symposium on Biomedical Imaging: From Nano to Macro*, pp. 1339–1342, 2008.
- [6] J. Chao et. al., "A resolution measure for three-dimensional microscopy," *Opt. Commun.*, vol. 282, pp. 1751–1761, 2009.
- [7] M. Born and E. Wolf, *Principles of Optics*, Cambridge University Press, Cambridge, UK, 1999.
- [8] S. Ram et. al., "How accurately can a single molecule be localized in three dimensions using a fluorescence microscope?" *Proc. SPIE*, vol. 5699, pp. 426–435, 2005.